Detection of the ISW effect and corresponding dark energy constraints

(astro-ph/0602398)

Jason McEwen[1]

with P. Vielva[2,3], M. P. Hobson[1], E. Martinez-González[2] and A. N. Lasenby[1]

[1]Cavendish Laboratory, University of Cambridge
[2]Instituto de Física de Cantabria, Universidad de Cantabria
[3]Laboratoire APC, Collège de France

IoA, Cambridge :: 5 July 2006

Outline

Outline

ISW effect
Physical origin

- Late ISW effect
  - CMB photons blue (red) shifted when fall into (out of) potential wells
  - Evolution of potential during photon propagation
    $\longrightarrow$ net change in photon energy
  - Gravitation potentials constant w.r.t. co-moving coordinates in matter dominated universe
  - Deviation from matter domination due to curvature or dark energy causes potentials to evolve with time
    $\longrightarrow$ secondary anisotropy induced in CMB
- WMAP shown universe is (nearly) flat
  detection of ISW effect $\longrightarrow$ direct evidence for dark energy
- Large scale phenomenon
  cosmic variance limited $\longrightarrow$ require full-sky maps

ISW effect
Physical origin

- Late ISW effect
  - CMB photons blue (red) shifted when fall into (out of) potential wells
  - Evolution of potential during photon propagation
    $\longrightarrow$ net change in photon energy
  - Gravitation potentials constant w.r.t. co-moving coordinates in matter dominated universe
  - Deviation from matter domination due to curvature or dark energy causes potentials to evolve with time
    $\longrightarrow$ secondary anisotropy induced in CMB
- WMAP shown universe is (nearly) flat
  detection of ISW effect $\longrightarrow$ direct evidence for dark energy
- Large scale phenomenon
  cosmic variance limited $\longrightarrow$ require full-sky maps

ISW effect
Physical origin

- Late ISW effect
  - CMB photons blue (red) shifted when fall into (out of) potential wells
  - Evolution of potential during photon propagation
    $\longrightarrow$ net change in photon energy
  - Gravitation potentials constant w.r.t. co-moving coordinates in matter dominated universe
  - Deviation from matter domination due to curvature or dark energy causes potentials to evolve with time
    $\longrightarrow$ secondary anisotropy induced in CMB
- WMAP shown universe is (nearly) flat
  detection of ISW effect $\rightarrow$ direct evidence for dark energy
- Large scale phenomenon
  cosmic variance limited $\rightarrow$ require full-sky maps

Detecting the ISW effect

Cross-correlating the CMB with LSS

- Cannot directly separate the ISW signal from CMB anisotropies
- Detected by cross-correlating CMB anisotropies with tracers of large scale structure (Crittenden & Turok 1996)
- Detections used to place constraints on dark energy (independent evidence for dark energy)
- Previous works
  - Real space angular correlation function (e.g. Boughn & Crittenden 2002, 2004)
  - Harmonic space cross-angular power spectrum (e.g. Afshordi et al. 2004)
  - Azimuthally symmetric wavelet covariance (Vielva et al. 2006)
- We extend spherical wavelet approach to directional wavelets (expect non-azimuthally symmetric local structures)

Detecting the ISW effect

Cross-correlating the CMB with LSS

- Cannot directly separate the ISW signal from CMB anisotropies
- Detected by cross-correlating CMB anisotropies with tracers of large scale structure (Crittenden & Turok 1996)
- Detections used to place constraints on dark energy (independent evidence for dark energy)
- Previous works
  - Real space angular correlation function (e.g. Boughn & Crittenden 2002, 2004)
  - Harmonic space cross-angular power spectrum (e.g. Afshordi et al. 2004)
  - Azimuthally symmetric wavelet covariance (Vielva et al. 2006)
- We extend spherical wavelet approach to directional wavelets (expect non-azimuthally symmetric local structures)

Detecting the ISW effect

Cross-correlating the CMB with LSS

- Cannot directly separate the ISW signal from CMB anisotropies
- Detected by cross-correlating CMB anisotropies with tracers of large scale structure (Crittenden & Turok 1996)
- Detections used to place constraints on dark energy (independent evidence for dark energy)
- Previous works
  - Real space angular correlation function (e.g. Boughn & Crittenden 2002, 2004)
  - Harmonic space cross-angular power spectrum (e.g. Afshordi et al. 2004)
  - Azimuthally symmetric wavelet covariance (Vielva et al. 2006)
- We extend spherical wavelet approach to directional wavelets (expect non-azimuthally symmetric local structures)

Detecting the ISW effect

Cross-correlating the CMB with LSS

- Cannot directly separate the ISW signal from CMB anisotropies
- Detected by cross-correlating CMB anisotropies with tracers of large scale structure (Crittenden & Turok 1996)
- Detections used to place constraints on dark energy (independent evidence for dark energy)
- Previous works
  - Real space angular correlation function (e.g. Boughn & Crittenden 2002, 2004)
  - Harmonic space cross-angular power spectrum (e.g. Afshordi et al. 2004)
  - Azimuthally symmetric wavelet covariance (Vielva et al. 2006)
- We extend spherical wavelet approach to directional wavelets (expect non-azimuthally symmetric local structures)

Detecting the ISW effect

Cross-correlating the CMB with LSS

- Cannot directly separate the ISW signal from CMB anisotropies
- Detected by cross-correlating CMB anisotropies with tracers of large scale structure (Crittenden & Turok 1996)
- Detections used to place constraints on dark energy (independent evidence for dark energy)
- Previous works
  - Real space angular correlation function (e.g. Boughn & Crittenden 2002, 2004)
  - Harmonic space cross-angular power spectrum (e.g. Afshordi et al. 2004)
  - Azimuthally symmetric wavelet covariance (Vielva et al. 2006)
- We extend spherical wavelet approach to directional wavelets (expect non-azimuthally symmetric local structures)

Outline

Spherical wavelet transform

Anisotropic dilation on the sphere

- Spherical wavelet transform (Antoine and Vandergheynst 1998; Wiaux et al. 2005)
- Stereographic projection Π
- Anisotropic dilation on the sphere

$$\mathcal{D}(a,b) = \Pi^{-1}\, d(a,b)\, \Pi$$

$$[\mathcal{D}(a,b)s](\omega) = [\lambda(a,b,\theta,\phi)]^{1/2}\, s(\omega_{1/a,1/b})$$

where

$\omega_{a,b} = (\theta_{a,b}, \phi_{a,b})$,

$\tan(\theta_{a,b}/2) = \tan(\theta/2)\sqrt{a^2\cos^2\phi + b^2\sin^2\phi}$

$\tan(\phi_{a,b}) = \frac{b}{a}\tan(\phi)$

Spherical wavelet transform
Anisotropic dilation on the sphere

- Spherical wavelet transform (Antoine and Vandergheynst 1998; Wiaux et al. 2005)
- Stereographic projection Π
- Anisotropic dilation on the sphere

$$\mathcal{D}(a,b) = \Pi^{-1}\, d(a,b)\, \Pi$$

$$[\mathcal{D}(a,b)s](\omega) = [\lambda(a,b,\theta,\phi)]^{1/2}\, s(\omega_{1/a,1/b})$$

where

$\omega_{a,b} = (\theta_{a,b}, \phi_{a,b})$,

$\tan(\theta_{a,b}/2) = \tan(\theta/2)\sqrt{a^2\cos^2\phi + b^2\sin^2\phi}$

$\tan(\phi_{a,b}) = \frac{b}{a}\tan(\phi)$

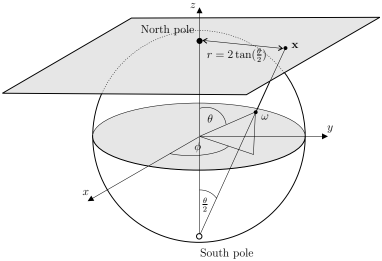

Spherical wavelet transform

Anisotropic dilation on the sphere

- Spherical wavelet transform (Antoine and Vandergheynst 1998; Wiaux et al. 2005)
- Stereographic projection Π
- Anisotropic dilation on the sphere

$$\mathcal{D}(a,b) = \Pi^{-1}\, d(a,b)\, \Pi$$

$$[\mathcal{D}(a,b)s](\omega) = [\lambda(a,b,\theta,\phi)]^{1/2}\, s(\omega_{1/a,1/b})$$

where

$$\omega_{a,b} = (\theta_{a,b}, \phi_{a,b}),$$
$$\tan(\theta_{a,b}/2) = \tan(\theta/2)\sqrt{a^2\cos^2\phi + b^2\sin^2\phi}$$
$$\tan(\phi_{a,b}) = \frac{b}{a}\tan(\phi)$$

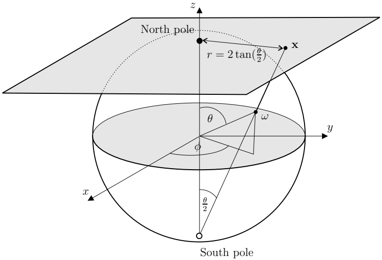

Spherical wavelet transform

Mother wavelets on the sphere

- Stereographic projection of admissible Euclidean mother wavelets

$$\psi(\omega) = [\Pi^{-1} \psi_{\mathbb{R}^2}](\omega)$$

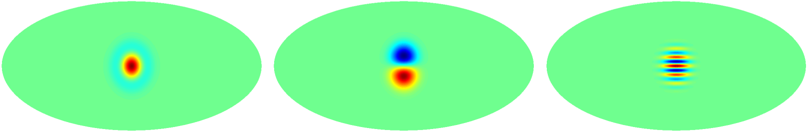

(a) SMHW (b) SBW (c) SMW

Figure: Spherical wavelets at scale $a = b = 0.2$.

Spherical wavelet transform

- Motion on the sphere ($\equiv$ rotation)

$$[R(\rho)s](\omega) = s(\rho^{-1}\omega), \quad \rho \in \mathrm{SO}(3)$$

- Multi-resolution basis on the sphere

$$\{\psi_{a,b,\rho} \equiv R(\rho)\mathcal{D}(a,b)\psi; \;\; \rho \in \mathrm{SO}(3); \; a,b \in \mathbb{R}_*^+\}$$

- Spherical wavelet transform

$$W_\psi(a,b,\rho) \equiv \int_{S^2} \mathrm{d}\Omega(\omega)\, \psi_{a,b,\rho}^*(\omega)\, s(\omega)$$

- Fast algorithm (McEwen et al. 2005; Wandelt & Gorski 2001)

Spherical wavelet transform

- Motion on the sphere ($\equiv$ rotation)

$$[R(\rho)s](\omega) = s(\rho^{-1}\omega), \quad \rho \in \mathrm{SO}(3)$$

- Multi-resolution basis on the sphere

$$\{\psi_{a,b,\rho} \equiv R(\rho)\mathcal{D}(a,b)\psi;\ \rho \in \mathrm{SO}(3);\ a,b \in \mathbb{R}_*^+\}$$

- Spherical wavelet transform

$$W_\psi(a,b,\rho) \equiv \int_{S^2} \mathrm{d}\Omega(\omega)\, \psi_{a,b,\rho}^*(\omega)\, s(\omega)$$

- Fast algorithm (McEwen et al. 2005; Wandelt & Gorski 2001)

Spherical wavelet transform

- Motion on the sphere ($\equiv$ rotation)

$$[R(\rho)s](\omega) = s(\rho^{-1}\omega), \quad \rho \in \mathrm{SO}(3)$$

- Multi-resolution basis on the sphere

$$\{\psi_{a,b,\rho} \equiv R(\rho)\mathcal{D}(a,b)\psi; \ \rho \in \mathrm{SO}(3); \ a, b \in \mathbb{R}_*^+\}$$

- Spherical wavelet transform

$$W_\psi(a,b,\rho) \equiv \int_{S^2} \mathrm{d}\Omega(\omega)\, \psi_{a,b,\rho}^*(\omega)\, s(\omega)$$

- Fast algorithm (McEwen et al. 2005; Wandelt & Gorski 2001)

Spherical wavelet transform

- Motion on the sphere ($\equiv$ rotation)

$$[R(\rho)s](\omega) = s(\rho^{-1}\omega), \quad \rho \in \mathrm{SO}(3)$$

- Multi-resolution basis on the sphere

$$\{\psi_{a,b,\rho} \equiv R(\rho)\mathcal{D}(a,b)\psi; \ \rho \in \mathrm{SO}(3); \ a,b \in \mathbb{R}_*^+\}$$

- Spherical wavelet transform

$$W_\psi(a,b,\rho) \equiv \int_{S^2} \mathrm{d}\Omega(\omega)\, \psi^*_{a,b,\rho}(\omega)\, s(\omega)$$

- Fast algorithm (McEwen et al. 2005; Wandelt & Gorski 2001)

Outline

Wavelet covariance estimator

- Wavelet covariance

$$\hat{X}_\psi^{\mathrm{NT}}(a,b,\gamma) = \frac{1}{N_{\alpha\beta}} \sum_{\alpha,\beta} \nu_{\alpha\beta} \, W_\psi^{\mathrm{N}}(a,b,\alpha,\beta,\gamma) \, W_\psi^{\mathrm{T}}(a,b,\alpha,\beta,\gamma)$$

- Average over orientations

$$\hat{X}_\psi^{\mathrm{NT}}(a,b) = \frac{1}{N_\gamma} \sum_{\gamma} \hat{X}_\psi^{\mathrm{NT}}(a,b,\gamma)$$

- Theoretical wavelet covariance

$$X_\psi^{\mathrm{NT}}(a,b,\gamma) = \sum_{\ell=0}^{\infty} {p_\ell}^2 \, b_\ell^{\mathrm{N}} \, b_\ell^{\mathrm{T}} \, C_\ell^{\mathrm{NT}} \sum_{m=-\ell}^{\ell} |(\psi_{a,b})_{\ell m}|^2$$

Wavelet covariance estimator

- Wavelet covariance

$$\hat{X}_\psi^{\mathrm{NT}}(a,b,\gamma) = \frac{1}{N_{\alpha\beta}} \sum_{\alpha,\beta} \nu_{\alpha\beta}\, W_\psi^{\mathrm{N}}(a,b,\alpha,\beta,\gamma)\, W_\psi^{\mathrm{T}}(a,b,\alpha,\beta,\gamma)$$

- Average over orientations

$$\hat{X}_\psi^{\mathrm{NT}}(a,b) = \frac{1}{N_\gamma} \sum_{\gamma} \hat{X}_\psi^{\mathrm{NT}}(a,b,\gamma)$$

- Theoretical wavelet covariance

$$X_\psi^{\mathrm{NT}}(a,b,\gamma) = \sum_{\ell=0}^{\infty} {p_\ell}^2\, b_\ell^{\mathrm{N}}\, b_\ell^{\mathrm{T}}\, C_\ell^{\mathrm{NT}} \sum_{m=-\ell}^{\ell} |(\psi_{a,b})_{\ell m}|^2$$

Wavelet covariance estimator

- Wavelet covariance

$$\hat{X}_{\psi}^{\mathrm{NT}}(a,b,\gamma) = \frac{1}{N_{\alpha\beta}} \sum_{\alpha,\beta} \nu_{\alpha\beta}\, W_{\psi}^{\mathrm{N}}(a,b,\alpha,\beta,\gamma)\, W_{\psi}^{\mathrm{T}}(a,b,\alpha,\beta,\gamma)$$

- Average over orientations

$$\hat{X}_{\psi}^{\mathrm{NT}}(a,b) = \frac{1}{N_{\gamma}} \sum_{\gamma} \hat{X}_{\psi}^{\mathrm{NT}}(a,b,\gamma)$$

- Theoretical wavelet covariance

$$X_{\psi}^{\mathrm{NT}}(a,b,\gamma) = \sum_{\ell=0}^{\infty} {p_{\ell}}^2\, b_{\ell}^{\mathrm{N}}\, b_{\ell}^{\mathrm{T}}\, C_{\ell}^{\mathrm{NT}} \sum_{m=-\ell}^{\ell} |(\psi_{a,b})_{\ell m}|^2$$

Comparison of wavelets

- Compare predicted signal-to-noise ratio

$$\mathrm{SNR}_\psi(a,b) = \frac{\left\langle \hat{X}_\psi^{\mathrm{NT}}(a,b) \right\rangle}{\Delta \hat{X}_\psi^{\mathrm{NT}}(a,b)}$$

where

$$\left[\Delta \hat{X}_\psi^{\mathrm{NT}}(a,b)\right]^2 = \sum_{\ell=0}^{\infty} \frac{1}{2\ell+1} \, {p_\ell}^4 \, (b_\ell^{\mathrm{N}})^2 \, (b_\ell^{\mathrm{T}})^2 \left[\sum_{m=-\ell}^{\ell} \left| (\psi_{a,b})_{\ell m} \right|^2 \right]^2 \left[(C_\ell^{\mathrm{NT}})^2 + C_\ell^{\mathrm{TT}} C_\ell^{\mathrm{NN}} \right]$$

- Similar technique used to compare real, harmonic and wavelet space techniques for detection of cross-correlations
  $\longrightarrow$ wavelets optimal on certain scales (Vielva et al. 2006)

Comparison of wavelets

- Compare predicted signal-to-noise ratio

$$\mathrm{SNR}_\psi(a,b) = \frac{\left\langle \hat{X}_\psi^{\mathrm{NT}}(a,b) \right\rangle}{\Delta \hat{X}_\psi^{\mathrm{NT}}(a,b)}$$

where

$$\left[\Delta \hat{X}_\psi^{\mathrm{NT}}(a,b)\right]^2 = \sum_{\ell=0}^{\infty} \frac{1}{2\ell+1}\, {p_\ell}^4\, (b_\ell^{\mathrm{N}})^2\, (b_\ell^{\mathrm{T}})^2 \left[\sum_{m=-\ell}^{\ell} \left|(\psi_{a,b})_{\ell m}\right|^2\right]^2 \left[(c_\ell^{\mathrm{NT}})^2 + c_\ell^{\mathrm{TT}} c_\ell^{\mathrm{NN}}\right]$$

- Similar technique used to compare real, harmonic and wavelet space techniques for detection of cross-correlations
$\rightarrow$ wavelets optimal on certain scales (Vielva et al. 2006)

Comparison of wavelets
SNR plots

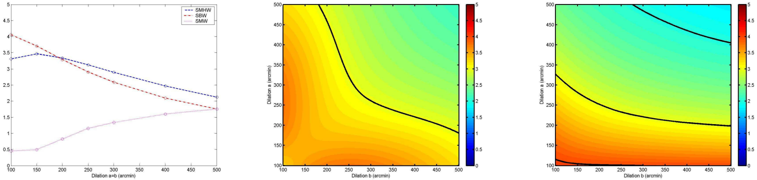

(a) All wavelets (b) SMHW (c) SBW

Figure: Expected SNR of the wavelet covariance estimator of CMB and radio source maps

- Don't consider SMW further
  (actually considered; as expected not effective)

Comparison of wavelets

SNR plots

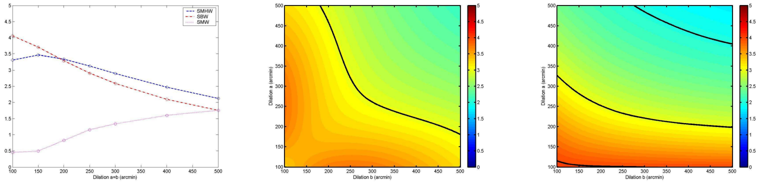

(a) All wavelets (b) SMHW (c) SBW

Figure: Expected SNR of the wavelet covariance estimator of CMB and radio source maps

- Don't consider SMW further
  (actually considered; as expected not effective)

Outline

Analysis procedure

- Data

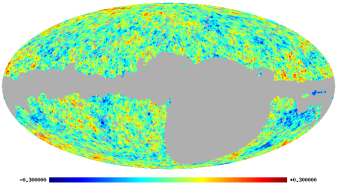

WMAP1

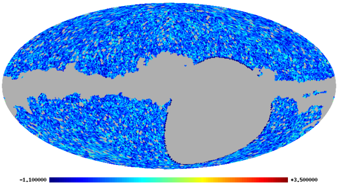

NVSS

- Analysis (scales; masks)
- Simulations
- Constraints on dark energy parameters

Analysis procedure

- Data

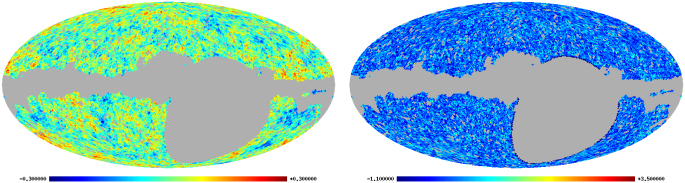

WMAP1 NVSS

- Analysis (scales; masks)
- Simulations
- Constraints on dark energy parameters

Analysis procedure

- Data

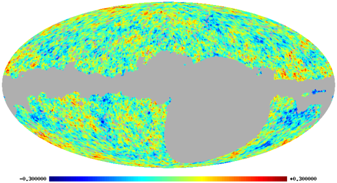

WMAP1

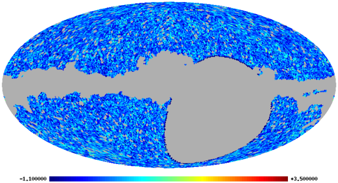

NVSS

- Analysis (scales; masks)
- Simulations
- Constraints on dark energy parameters

Analysis procedure

- Data

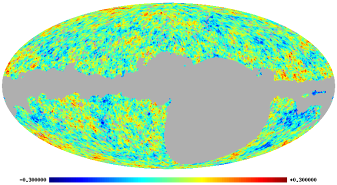

WMAP1

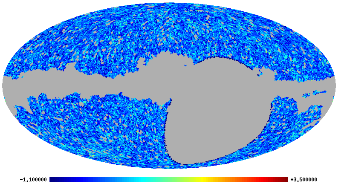

NVSS

- Analysis (scales; masks)
- Simulations
- Constraints on dark energy parameters

Outline

Scales and detections

- Scales

Scale	1	2	3	4	5	6	7
Dilation a	$100'$	$150'$	$200'$	$250'$	$300'$	$400'$	$500'$
Size on sky 1	$282'$	$424'$	$565'$	$706'$	$847'$	$1130'$	$1410'$
Size on sky 2	$31.4'$	$47.1'$	$62.8'$	$78.5'$	$94.2'$	$126'$	$157'$

- Wavelet covariance plots

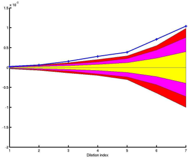

SMHW

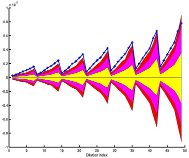

SMHW

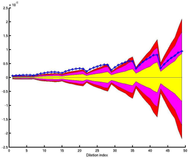

SBW

Significance of detections

- Most significant detections
  - Wavelet covariance statistics appear Gaussian
    $\rightarrow N_\sigma$ direct indication of significance of detections
  - symmetric SMHW: 3.6σ; elliptical SMHW: 3.9σ; SBW: 3.9σ
- N_σ plots (2 and 3σ contours)

Significance of detections

- Most significant detections
  - Wavelet covariance statistics appear Gaussian
    $\rightarrow N_\sigma$ direct indication of significance of detections
  - symmetric SMHW: 3.6σ; elliptical SMHW: 3.9σ; SBW: 3.9σ
- N_σ plots (2 and 3σ contours)

Significance of detections

- Most significant detections
  - Wavelet covariance statistics appear Gaussian
    $\rightarrow N_\sigma$ direct indication of significance of detections
  - symmetric SMHW: 3.6σ; elliptical SMHW: 3.9σ; SBW: 3.9σ
- N_σ plots (2 and 3σ contours)

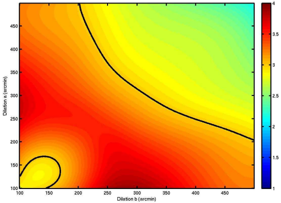

SMHW

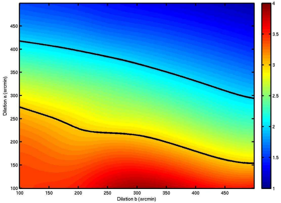

SBW

Systematics and foregrounds

- Systematics: individual WMAP receiver maps
  $\longrightarrow$ systematics not likely source of detection
- Foregrounds: foreground dominated difference maps
  $\longrightarrow$ foregrounds not likely source of detection

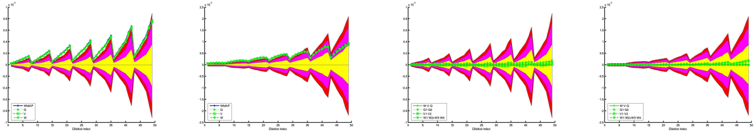

SMHW SBW SMHW SBW

Individual receiver maps — Difference maps

Localised regions

Detection

- Wavelets inherently provide spatial localisation (in addition to scale localisation)
- Threshold wavelet coefficient product maps to localise most likely sources

Localised regions
Detection

- Wavelets inherently provide spatial localisation (in addition to scale localisation)
- Threshold wavelet coefficient product maps to localise most likely sources

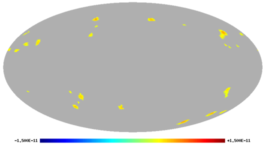

Symmetric SMHW

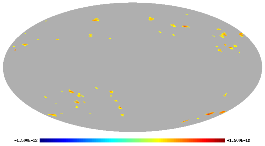

Elliptical SMHW

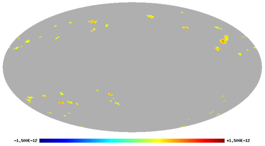

SBW

Localised regions
Removal

- Remove localised regions → ISW detection remains
  (Agrees with findings of Boughn and Crittenden 2004)

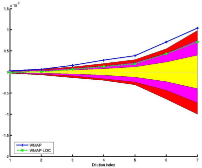

Symmetric SMHW

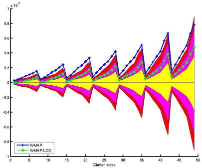

Elliptical SMHW

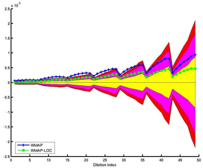

SBW

- Examined localised regions in closer detail

Dark energy constraints

- Compute theoretical wavelet covariance for models (w, Ω_Λ) (assume concordance model for other parameters; bias $b = 1.6$)
- Compare theoretical predictions with observations

$$\chi^2(w, \Omega_\Lambda) = \Delta^{\mathrm{T}} C^{-1} \Delta$$

where $$\Delta = [\hat{X}_\psi^{\mathrm{NT}}(a, b, \gamma) - X_\psi^{\mathrm{NT}}(a, b, \gamma | w, \Omega_\Lambda)]$$

- Compute likelihood

$$\mathcal{L}(w, \Omega_\Lambda) \propto \exp[-\chi^2(w, \Omega_\Lambda)/2]$$

Dark energy constraints

- Compute theoretical wavelet covariance for models (w, Ω_Λ)
  (assume concordance model for other parameters; bias $b = 1.6$)
- Compare theoretical predictions with observations

$$\chi^2(w, \Omega_\Lambda) = \Delta^{\mathrm{T}} C^{-1} \Delta$$

where $$\Delta = [\hat{X}_\psi^{\mathrm{NT}}(a, b, \gamma) - X_\psi^{\mathrm{NT}}(a, b, \gamma | w, \Omega_\Lambda)]$$

- Compute likelihood

$$\mathcal{L}(w, \Omega_\Lambda) \propto \exp[-\chi^2(w, \Omega_\Lambda)/2]$$

Dark energy constraints

- Compute theoretical wavelet covariance for models (w, Ω_Λ)
  (assume concordance model for other parameters; bias $b = 1.6$)
- Compare theoretical predictions with observations

$$\chi^2(w, \Omega_\Lambda) = \Delta^{\mathrm{T}} C^{-1} \Delta$$

where $$\Delta = [\hat{X}_\psi^{\mathrm{NT}}(a, b, \gamma) - X_\psi^{\mathrm{NT}}(a, b, \gamma | w, \Omega_\Lambda)]$$

- Compute likelihood

$$\mathcal{L}(w, \Omega_\Lambda) \propto \exp[-\chi^2(w, \Omega_\Lambda)/2]$$

Dark energy constraints

Likelihood surfaces

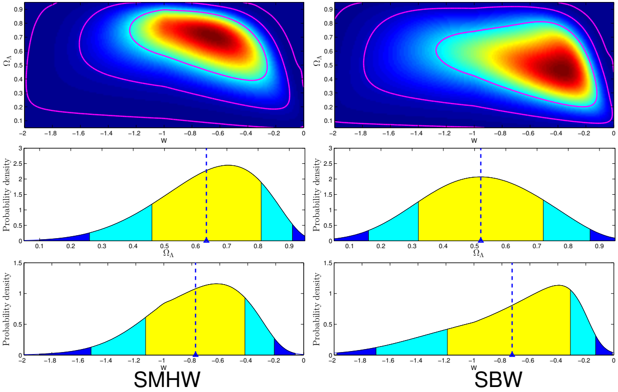

- Parameter estimates from mean of marginalised distributions
  - $\Omega_\Lambda = 0.63^{+0.18}_{-0.17}$; $w = -0.77^{+0.35}_{-0.36}$ using SMHW
  - $\Omega_\Lambda = 0.52^{+0.20}_{-0.20}$; $w = -0.73^{+0.42}_{-0.46}$ using SBW

Dark energy constraints

Likelihood surfaces

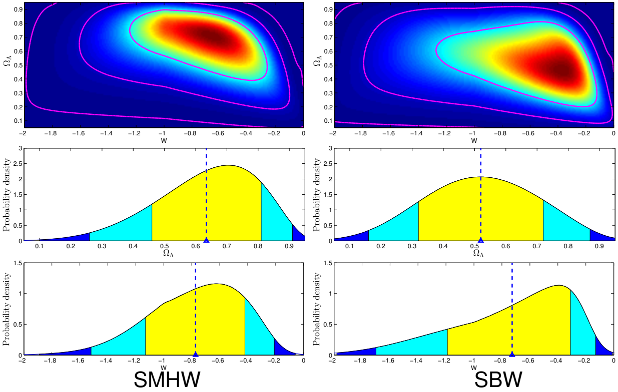

- Parameter estimates from mean of marginalised distributions
  - $\Omega_\Lambda = 0.63^{+0.18}_{-0.17}$; $w = -0.77^{+0.35}_{-0.36}$ using SMHW
  - $\Omega_\Lambda = 0.52^{+0.20}_{-0.20}$; $w = -0.73^{+0.42}_{-0.46}$ using SBW

Dark energy constraints

Parameter estimates

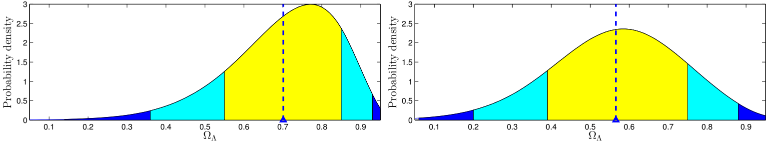

- Also considered case $w = -1$
  - $\Omega_\Lambda = 0.70^{+0.15}_{-0.15}$ using SMHW
  - $\Omega_\Lambda = 0.57^{+0.18}_{-0.18}$ using SBW
- Reject $\Omega_\Lambda = 0$ at $> 99\%$ significance
  - $\Omega_\Lambda > 0.1$ at 99.9% using SMHW
  - $\Omega_\Lambda > 0.1$ at 99.7% using SBW

Dark energy constraints

Parameter estimates

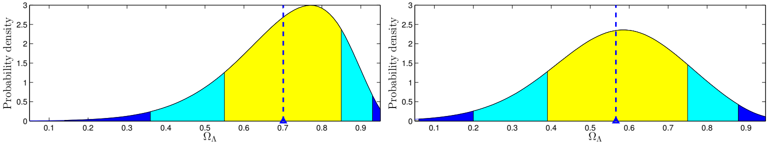

- Also considered case $w = -1$
  - $\Omega_\Lambda = 0.70^{+0.15}_{-0.15}$ using SMHW
  - $\Omega_\Lambda = 0.57^{+0.18}_{-0.18}$ using SBW
- Reject $\Omega_\Lambda = 0$ at $> 99\%$ significance
  - $\Omega_\Lambda > 0.1$ at 99.9% using SMHW
  - $\Omega_\Lambda > 0.1$ at 99.7% using SBW

Outline

Summary

- Spherical wavelets used to detect ISW effect
- Detection of ISW effect made at almost 4σ
- Independent evidence of dark energy
- Constraints on dark energy
  - Good consistency check with direct estimates from other approaches
  - Wavelets of similar performance for constraining dark energy as other ISW techniques